UIDE

Powered by
Arizona State University

ING. MECATRÓNICA

Tesis previa a la obtención del título de Ingeniero en Mecatrónica.

Autor: Bucheli Alemán, Anthony Ricardo

Tutor: Bonilla Venegas, Félix Vladimir

Diseño y construcción una estación autónoma de monitoreo par los glaciares del Ecuador

Design and construction of an autonomous system for glacier monitoring in Ecuador

Quito-2026

Approval of the Tutor of the Curricular Integration Work

I, Félix Vladimir Bonilla Egas, as tutor of the Curricular Integration Project entitled: DESIGN AND CONSTRUCTION OF AN AUTONOMOUS SYSTEM FOR GLACIER MONITORING IN ECUADOR, prepared by Anthony Ricardo Bucheli Alemán, have reviewed and supervised it in all its parts and consider that it meets the requirements established by the institution. Therefore, I give my approval for it to continue with the corresponding academic process.

Vladimir Bonilla

CERTIFICATE OF AUTHORSHIP

I, Anthony Bucheli, hereby declare that this submission is my own work, it has not been previously submitted for any degree or professional qualification and that the detailed bibliography has been consulted.

I transfer my intellectual property rights to the Universidad Internacional del Ecuador, to be published and divulged on the internet, according to the provisions of the Ley de Propiedad Intelectual, its regulations and other legal dispositions.

Anthony Bucheli

CONTENTS

LIST OF FIGURES

LIST OF TABLES

1. INTRODUCTION

The tropical glaciers of the Ecuadorian Andes act as highly sensitive barometers for climate change; their reaction to shifts in temperature and precipitation is immediate. On the Antisana volcano, specifically Glacier 15, research has observed a persistent loss of mass since the late 20th century. This process accelerates violently during El Niño events, while stabilizing only temporarily during La Niña years [2]. Long-term geodetic records confirm this trajectory: the Antisana ice cap shed approximately 42% of its surface area between 1956 and 2016, a reduction that mirrors the region's progressive warming [3].

However, the most alarming indicator is the Carihuairazo volcano. Between September 2023 and January 2024, its glacier did not merely retreat; it effectively collapsed, shrinking from 1312.5 m^2 to less than 101 m^2 [4]. By definition, this constitutes total extinction. Such rapid loss exposes the extreme vulnerability of the Ecuadorian cryosphere and highlights a critical operational gap, the lack of continuous data. While empirical models confirm that variables like air temperature and wind speed drive glacial retreat [5], and specific studies on Antisana 12 assess meltwater contributions to nearby basins [6], current understanding is fragmented. Most measurements rely on isolated stations or sporadic campaigns, limiting the ability to capture the dynamic behavior of these disappearing ecosystems.

Existing solutions in this field generally fall into two categories: pure glaciological analysis and general-purpose IoT development.

In the glaciological domain, significant effort has focused on the Antisana ice cap. These studies analyze mass balance, climate variability, and surface area evolution [2]. notably, decade-by-decade analyses have successfully demonstrated how topography and regional climatic conditions dictate changes in ice sheet volume [3]. Similarly, research centered on Antisana 12 has provided detailed insights into the link between climate, ice melt, and downstream water availability [6].

In parallel, the field of instrumentation has matured substantially. Specialized reviews

of IoT sensor technologies reveal a landscape now populated by low-power, high- accuracy components specifically adaptable to remote microcontrollers [7]. Modern architectures for these systems have shifted focus, prioritizing energy efficiency and the absolute integrity of the data stream [8]. Similar obstacles regarding the maintenance of sensor accuracy under fluctuating conditions have been mirrored in the environmental water management sector [9].

Yet, a significant gap remains when merging these technological advances with the hostility of a tropical glacier. The Andean context is unforgiving; sub-zero temperatures, violent weather shifts, intense solar radiation, and pervasive humidity conspire to degrade standard equipment rapidly. Consequently, the engineering of an autonomous system capable of withstanding these specific stressors constitutes a distinct and necessary contribution to the field.

Technologically, this project bridges the gap by integrating low-power embedded systems with calibratable sensors and MPPT-regulated solar power, complying with recent recommendations in environmental IoT [7], [8]. The social relevance is immediate: continuous, reliable data strengthens climate models and aids water resource planning for cities like Quito, which relies partially on glacial melt [5]. Ultimately, by functioning as a replicable prototype, the system offers a practical, robust tool for universities and institutions dedicated to monitoring these fragile ecosystems.

General objective

To design and implement an autonomous monitoring system for the continuous observation of high-altitude ecosystems in Ecuador, utilizing solar panels, IoT connectivity through WIFI, and internal data storage with periodic data transmission to the cloud, ensuring reliable, scalable, and sustainable operation.

Specific objectives

- Design a circuit with a minimum autonomy of 30 days to allow continuous environmental data collection without requiring frequent maintenance in high-altitude conditions.
- Implement a waterproof mechanical design that withstands low temperatures,

capable of protecting the monitoring system from damage caused by moisture and water exposure to the glacial environment.

- Integrate sensors to collect data on three critical variables: humidity, solar radiation, and temperature, which are essential for monitoring the conditions impacting glacial mass.
- Implement a data storage system with sufficient capacity to support at least 30 days of continuous data collection without saturation, ensuring data availability for later analysis.

2. Methodology

The autonomous monitoring system was designed following the V-model methodology, as defined by the German guideline VDI 2206 [1], a recognized general reference framework for the systematic design of mechatronic systems.

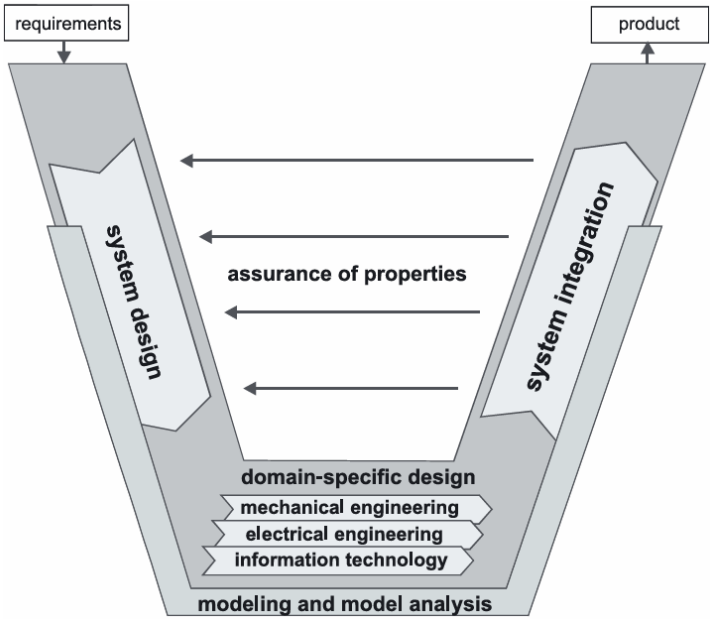

Figure 1. V-model for mechatronic system development according to VDI 2206. Adapted from [1].

This methodology provides a structured process that integrates mechanical, electronic, and software development while ensuring traceability between requirements, design stages, and validation activities.

According to VDI 2206, the V-model divides the development process into two main branches. The left-hand branch signifies system definition and design phases, starting with the requirement specification and going through functional, logical, and physical design. The right hand branch focuses on integration, verification, and validation, where each development stage is checked against its related design definition. This checked and the behavior of the system remains consistent with the initial requirements.

In this project, the V-model was applied by establishing functional requirements, non-functional requirements, and constraints that delineate the operational objectives, performance expectations, and environmental limitations of the monitoring station. Such requirements developed the base for the conceptual design to be established, followed by the specification of the functional, logical, and physical architectures. Each level of architecture addresses another abstraction layer of the system according to recommendations of VDI 2206 on how to manage system complexity.

Once all design stages were completed, implementation and integration activities took place on the right-hand side of the V-model. The various components and sub-systems-power train, sensing modules, embedded controller, local storage, and communication interface-were first tested in isolation and then integrated into the complete prototype. Verification at each level assured that the implemented system met the respective design specifications, whereas the system-level validation involved the testing of overall functionality, energy autonomy, as well as operational stability.

The adoption of the V-model according to VDI 2206 permitted a disciplined and traceable development process, reduced the integration risks, and allowed a clear transition from system requirements to a functional prototype. Embedded systems working in harsh environments, such as the case of high-altitude monitoring stations, require an approach that ensures reliability, robustness, and systematic validation.

2.1. Requirements

To ensure the system's viability in the hostile environment of high-altitude ecosystems, the following requirements were established based on the operational gaps identified

in the problem definition.

Functional Requirements

- **Configurable Data Acquisition:** The core function is the periodic logging of environmental variables, specifically temperature, humidity, and radiation. The sampling interval must be user-configurable to balance data resolution with energy conservation.
- **Local Storage:** To mitigate the risk of data loss during inevitable connectivity blackouts, local non-volatile storage is mandatory for all captured records.
- **Automatic Synchronization:** Upon detection of an active Wi-Fi link, the device is required to autonomously trigger a synchronization process, uploading stored records to the designated cloud platform.
- **Energy Management and Preservation:** The system must perform self-monitoring of battery voltage. Based on this status, it is required to regulate its duty cycles, toggling between active and deep sleep states, to maximize operational lifespan.

Non-Functional Requirements

- **Energy Efficiency:** Power consumption must be minimized. The design requires the implementation of deep-sleep modes to reduce quiescent current, ensuring extended autonomy without frequent maintenance.
- **Portability:** Given the logistical difficulty of accessing the glacier, the physical prototype must maintain a compact and lightweight form factor to facilitate manual transport to high-altitude sites.

Constraints

- **Thermal Resilience:** The electronics and power systems must remain operational in ambient temperatures that consistently drop below 0°C.

- **Environmental Hardening:** The enclosure and external sensors are required to withstand direct exposure to the intense UV radiation characteristic of altitudes exceeding 4500 meters above sea level.

2.2. Conceptual design

The conceptual design consists of six main subsystems as shown in *Figure 1*.

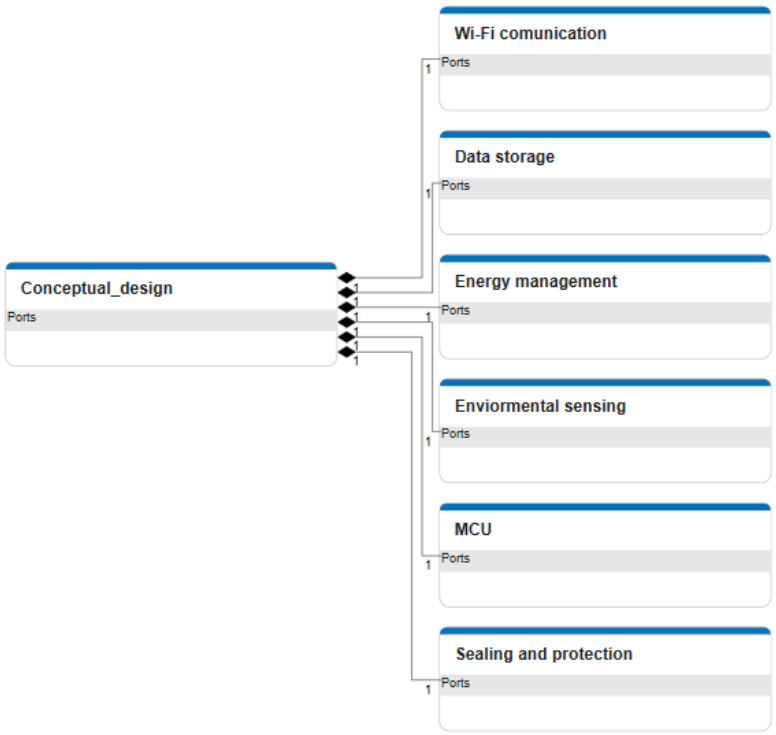

Figure 2. Conceptual design block diagram

WiFi communication: Functioning as the system's external interface, this module orchestrates the synchronization of local records with the cloud platform. Operation is opportunistic: transmission triggers strictly upon the detection of a viable connection. For the scope of this specific prototype, connectivity is restricted to the Wi-Fi infrastructure present at the validation site. Conceptually, this subsystem establishes the data egress path, transforming isolated internal logs into accessible information for external processing.

Data storage: Physically implemented via a microSD interface, this module serves as the local persistence layer. Its function is to archive measured data in a structured format, ensuring retention even during complete power loss. Conceptually, it acts as the

system's *black box* by creating a permanent, non-volatile backup of every reading, the module insulates the project from data loss caused by connectivity gaps or unexpected energy depletion

Energy management: Ensuring operational independence, the power subsystem manages the entire energy lifecycle. It integrates a photovoltaic panel for generation, coupled with a charge controller utilizing Maximum Power Point Tracking (MPPT) to optimize harvesting efficiency. A rechargeable battery acts as the storage buffer. Conceptually, this block functions as the autonomous supply backbone, delivering regulated power to both the microcontroller and the peripheral sensor array.

Environmental sensing: This subsystem aggregates the primary data acquisition hardware. Specifically, the design targets three critical environmental variables:

- Ambient temperature
- Relative humidity
- Solar radiation

The latter derived indirectly by monitoring the wattage yield of the photovoltaic panel. Interfaced with the microcontroller via digital buses, these components perform the fundamental physical-to-digital transduction. Their role is to convert raw environmental states into discrete electrical signals that the embedded system can process and log.

MCU: Primarily, it executes periodic sensor polling, followed by immediate signal conditioning, basic filtering and scaling. Beyond acquisition, it governs the device's logic: determining the precise timing for data logging, initiating deep-sleep cycles to conserve power, and triggering cloud transmission. It also dictates the write protocols for the storage memory. Conceptually, this module operates as the 'brain,' physically connecting and logically managing every peripheral block.

Sealing and protection: Finally, the physical integration of all subsystems is achieved within a mechanical enclosure. Its primary function is shielding: protecting sensitive electronics from ingress by rain, glacial dust, and intense radiation. Structurally, the casing provides external mounting interfaces for the solar panel, antennas (GPS/ Communication), and the environmental sensor probe. Conceptually, this chassis ensures the prototype bridges the gap between electrical functionality and field deployability, guaranteeing mechanical viability in conditions analogous to a high-altitude glacier.

2.3. Specific design

Integration of functions with physical modules

To meet the requirements for sensing variables of interest and care of the prototype, the following modules and sensors were integrated.

- **Sensing:**
  - Temperature and humidity sensor with IP67 enclosure, for environmental variables. (SHT30)
  - Basic temperature and humidity sensor for internal monitoring of the prototype. (DHT22)
  - Current sensor, senses the current generated by the solar panel. (ACS712)
  - Voltage sensor, used to measure the voltage generated by the solar panel and the battery level. (FZO430)
- **Preprocessing and timestamp.-** Embedded directly within the ESP32 firmware, this routine executes the critical data serialization logic. It performs more than simple pass-through, it applies digital filtering to sanitize raw inputs, structures the payload, and appends necessary metadata tags. Ultimately, it packetizes the information for subsequent storage or transmission. Integral to this workflow is the Timebase. By leveraging the ESP32's internal *Real-Time Clock* (RTC), the system attaches a precise timestamp to every acquisition event. This synchro-

nization ensures the chronological fidelity of the registers, allowing for accurate historical analysis of the environmental data.

- **Local storage.-** The SPI MicroSD module serves as the system's fail-safe for data retention. Operating via the SPI interface, it commits processed records complete with their chronological timestamps directly to physical storage. This local archival strategy effectively immunizes the dataset against loss, ensuring that the continuity of the environmental record is preserved even during periods of total connectivity isolation.

- **Communication.-** Wireless connectivity is established through the ESP32's native Wi-Fi controller, which has been physically modified to bypass the PCB trace antenna. Instead, the system utilizes an external SMA antenna to significantly improve signal gain and range in obstructed environments. On the application layer, data egress is managed by an embedded HTTP client. This process is opportunistic, the client initiates a POST request to the target API exclusively when a valid internet gateway is detected, ensuring efficient power usage during disconnected states.

- **Power management.-** Serving as the coordinator of the system's electrical vitality, the Power Management block governs the energy flow. Its responsibilities are threefold: executing precise voltage conversion, regulating the battery charging profile, and performing diagnostics of the energy state. Architecturally, this module is not standalone; it is inextricably linked to the specific *Power train* topology defined in the physical design, ensuring that control logic aligns perfectly with hardware capabilities.

- **Health monitor.-** To ensure hardware longevity, the system maintains a continuous health monitoring. It actively tracks the battery temperature and *state of charge* SOC.

Power train design

As shown in *Table 1*, the power train integrates the solar panel, MPPT, battery, and regulation stages required for autonomous operation.

Table 1. Components and functions of the system's power train.

Component	**Function**	**Technical Justification**
Solar panel 15 W	Generate electrical energy from available solar radiation.	Provides sufficient power to recharge the battery even under low irradiance conditions typical of high-altitude environments.
MPPT charge controller	Optimize the energy transfer from the solar panel to the battery.	Tracks the maximum power point of the panel, maintaining efficiency even with cloud cover or rapid fluctuations in light intensity.
TVS diodes 18V / 6V	Provide overvoltage protection on both the panel line and the regulated supply line.	Prevent failures in buck converters and in the embedded system due to electrical transients or voltage surges.
$LiFePO_4$ 12 V / 6 Ah battery	Store energy and supply power during nighttime or low-radiation periods.	Lithium iron phosphate batteries offer high thermal stability, long lifespan, and good performance at low temperatures.
5V buck converter	Step down the battery voltage to 5V for specific modules.	Provides a stable regulated output regardless of battery charge level variations.
3.3V buck converter	Generate the required voltage for the microcontroller and sensors.	Ensures efficient and stable power delivery to low-voltage and sensitive electronic components.
N-Channel MOSFET (Si2300)	Switch and control the power delivered to specific modules.	Enables energy savings by powering subsystems only when needed.

Continued on next page

Component	**Function**	**Technical Justification**
Heating pads (as per thermal design)	Increase the internal temperature when the battery approaches unsafe thermal thresholds.	Prevents battery degradation and ensures stable operation under extremely low temperatures.
IP68 cable gland	Seal cable entry points to the enclosure.	Ensures protection against moisture, dust, and snow, maintaining the system's IP rating.
ABS or polycarbonate IP67 enclosure	House and protect all electronic components.	Withstands impact, moisture, and thermal variations typical of high-altitude environments.

Processing, control and storage

The processing architecture is anchored by the ESP32 DEVKIT. Acting as the central control unit, this microcontroller does not operate in isolation. To interface with the industrial SHT30 sensor, the design incorporates a MAX485 module; this component bridges the logic-level signals of the MCU with the robust RS485 differential standard required for long-distance cabling.

Connectivity is further reinforced by an external antenna to optimize Wi-Fi signal gain, while an optional GPS module provides geospatial context. Internally, the ESP32 orchestrates a complex multitasking workflow: it manages raw data acquisition and preprocessing, executes real-time energy diagnostics, and governs the deep-sleep logic to ensure survival. Finally, it handles the dual output paths: writing structured logs to the SPI MicroSD memory and executing HTTP transmissions.

Specific design integration

The integration of the specific design *Figure 2* involves unifying all the subsystems established in the logical, physical, and functional architectures into a coherent operational flow.

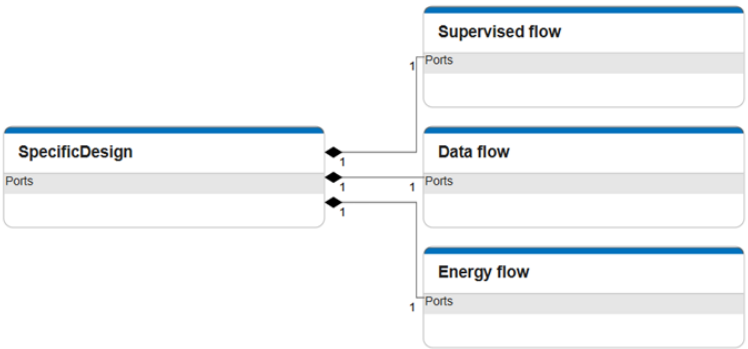

Figure 3. Specific design

Each module (communication, storage, power management, processing, and sensing) is connected in such a way that the physical signals, logical processes, and system functions interact in an organized manner. This integration ensures that the monitoring station completes its operational cycle by maintaining consistency between its operation and its actual implementation.

- **Data flow.-** The physical sensors for temperature, voltage, humidity, and current initiate the data flow. The values obtained are sent to the sensor abstraction module and then to the MCU for preprocessing. After organization, the data is split into two paths: local storage via the SPI MicroSD module and remote transmission via the HTTP client, which generates the API output to the server. This flow ensures data preservation even without connectivity and allows the structure established in the functional and logical architectures to be maintained.

- **Energy flow.-** Power travels from the solar panel to the MPPT (Maximum Power Point Tracker). The MPPT regulates the charge to the LiFePO4 battery. Power is then distributed from the battery to the 12 to 5V and 5 to 3.3V buck converters to power the MCU, peripherals, and sensors. Current and voltage sensing signals also originate from this power line, enabling safe and stable system control. This power path maintains device independence and adheres to the established physical architecture.

- **Supervised flow.-** The monitoring flow collects data about battery status, panel conditions, potential electrical faults, and the powertrain. This data is fed into the diagnostic module, where status indicators are created that the MCU interprets as part of its operational logic. This monitoring circuit enables the regulation of system behavior based on energy availability, hardware protection, and ensuring the reliability of transmitted data, thus preserving the consistency established in the logical and functional architectures.

Electronic circuit diagram

Figure 3 shows the complete electronic schematic of the autonomous monitoring system. The diagram integrates the power train, sensing modules, battery diagnostics, GPS module, local storage, and the ESP32 microcontroller.

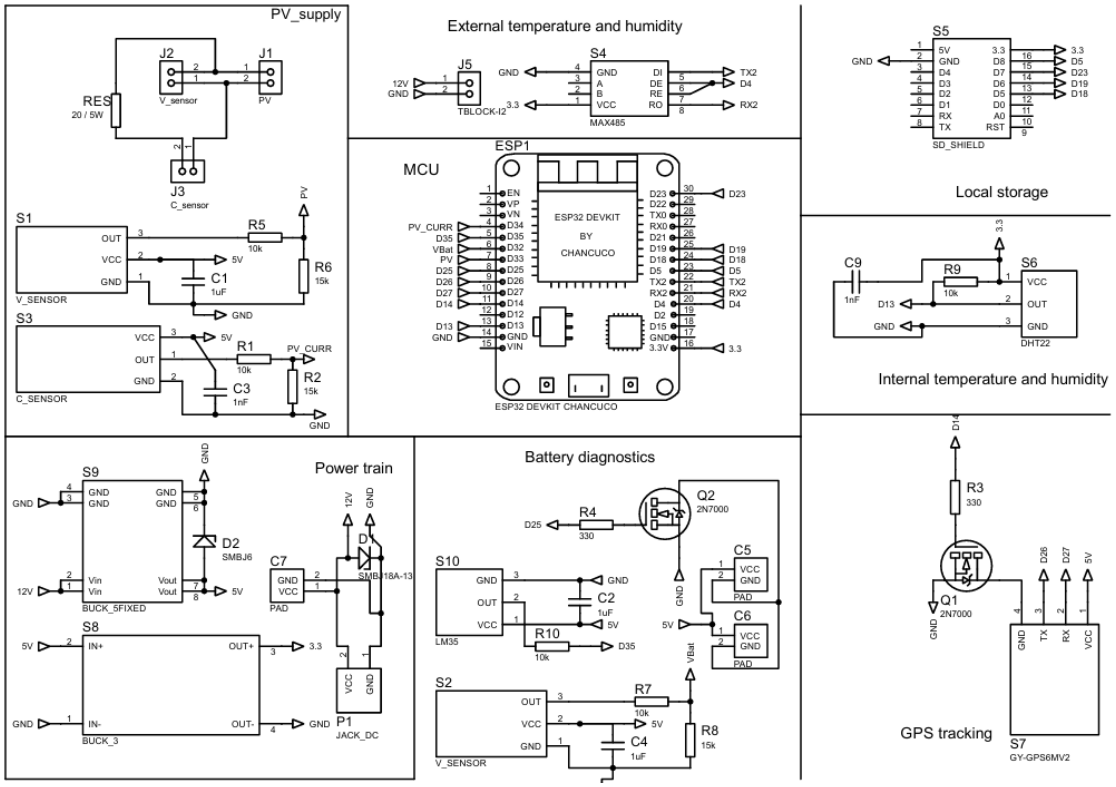

Figure 4. Complete electronic schematic of the autonomous monitoring system.

Figure 4 shows the hardware connection schematic of the prototype, which has two power supplies, one from the battery and the other from the photovoltaic panels. These supplies are switched with an output voltage of 14.6 V. From this node, two power lines are derived, supplying 5 V and 3.3 V as required by each component. Additionally, shocky TVS diodes were used on the 14.6 V and 5 V lines for equipment protection. The power train uses two voltage sensors and one current sensor. One voltage sensor measures the battery voltage, and the second sensor works in conjunction with the current sensor. This data is used to calculate the generated irradiance in W/m². For humidity and temperature measurements, the PLC's IP67 rated SHT30 sensor was used in conjunction with the MAX485 module for communication with the microcontroller. The DHT22 sensor measures the internal humidity and temperature of the prototype, the LM35 works in conjunction with the heating pads with a MOSFET to control the battery temperature, finally the microcontroller reads the sensed variables, establishes communication with the web terminal and stores these variables in the micro SD.

Operational Logic of the Embedded System

The developed prototype operational logic was designed to achieve robust performance, configurability, and to be highly energy-efficient during autonomous deployment. After system power-up, the WiFi Manager interface firstly allows the user to configure the operating mode and communication settings among other device parameters. In the configuration phase, there is set a time limit to prevent excessive energy waste.

If there is no user interaction or configuration within five minutes, the system automatically puts the ESP microcontroller into deep sleep for half an hour. When it wakes up, the same configuration loop repeats. This keeps going around in a cycle until it successfully configures, hence allowing efficient energy behavior during unattended deployment phases.

After configuration, the system can run in either of two modes:

- Datalogger mode.- Here, the system periodically reads sensor values and logs them locally. Following the data logging routine, the ESP goes into deep sleep mode for a user-configured period. This mode operates on very low power and stores data locally, making it appropriate for applications where network connectivity is scarce or unavailable.

- IoT mode.- In this setup, the user provides the network credentials and selects the deep sleep interval. The system then connects to the configured network, sends the gathered sensor data to a cloud, does local data logging as a backup, and then goes to deep sleep. This mode can enable remote monitoring with real-time access to data without wasting much energy. The system uses the non-volatile memory management of the Preferences.h library in both operating modes. This functionality lets the ESP maintain the selected configuration parameters during deep sleep cycles and power interruptions. Thus, following each wake-up event, the device enters operation using the previously stored configuration and there is no need for repetitive user intervention.

The flowchart in *Appendix 4* summarizes the overall system behavior and decision flow

by pictorially showing the configuration logic, the available operating modes, and the power management strategy deployed in the prototype.

3. Results

3.1. System integration

The integration phase represented the physical and logical convergence of distinct hardware modules into a unified entity. This process went beyond simple assembly; it demanded the electrical validation of the power backbone against the low-voltage logic of the ESP32, followed by the systematic flashing of the control firmware. Ultimately, the sensing units, local storage interface, and energy regulation circuits were consolidated within the mechanical enclosure, transitioning the project from a collection of disparate parts to a cohesive, field-ready prototype.

Assambly and hardware integration

Physical implementation commenced with the power train architecture. The solar panel, MPPT controller, and $LiFePO_4$ battery were interconnected with buck converters to establish the system's energy backbone. Crucially, the logic components, the ESP32, GPS, microSD interface, and the sensor array (SHT30, DHT22, ACS712, FZO430), were introduced only after the stability of the 5,V and 3.3,V rails was strictly verified. To mitigate integration risks, a modular validation strategy was adopted; each subsystem was tested in isolation before joining the main assembly. The process concluded with the calibration of sensor voltage dividers and the stress test of the full circuit, confirming the functionality of the power supply across all operational voltage lines as shown in *Figure 4*.

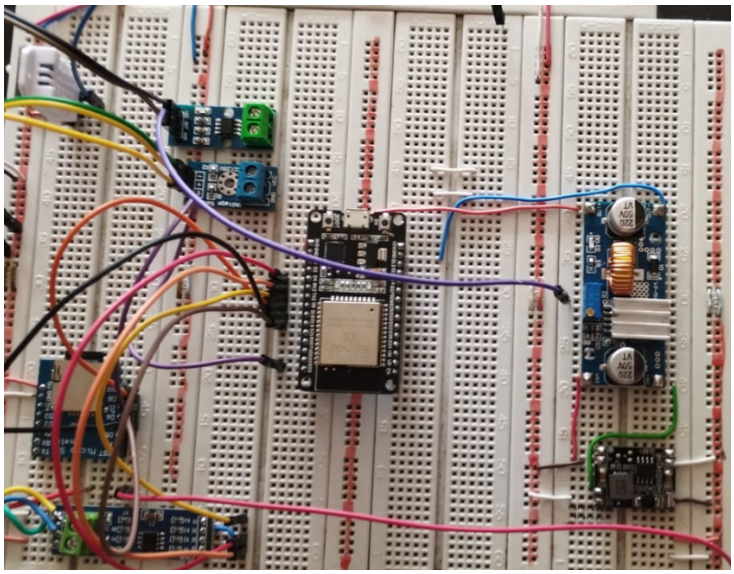

Figure 5. Operational voltage lines test

Once the correct functioning of the circuit was validated, the PCB was developed for its implementation as shown in *Figure 5*.

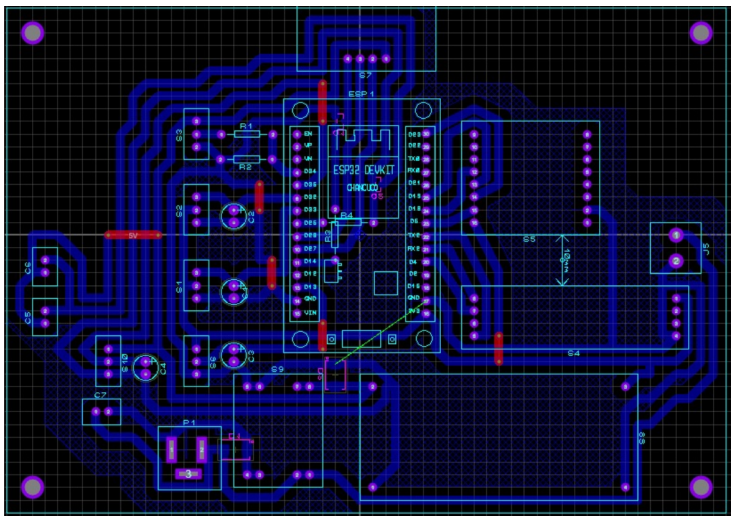

Figure 6. PCB v1

In this first version, the system worked correctly; however, the voltage and current sensors were powered by the 3.3V line to avoid using voltage dividers. This resulted in reading errors because voltages lower than 15V were used in the sensor calibration, and in tests with the PCB circuit, the panel was used with peak solar radiation exceeding 20V. The error lies in the fact that the signal generated by the voltage sensor exceeded 3.3V, and the ESP32 is incapable of reading voltages higher than this.

This problem was solved by changing the power supply line to 5V and adding a volt-

age divider to the sensors (ACS712, FZO430). Additionally, ceramic capacitors were added to the power supplies of each of the sensors as a precaution against the noise generated and to avoid false readings as shown in *Figure 6*.

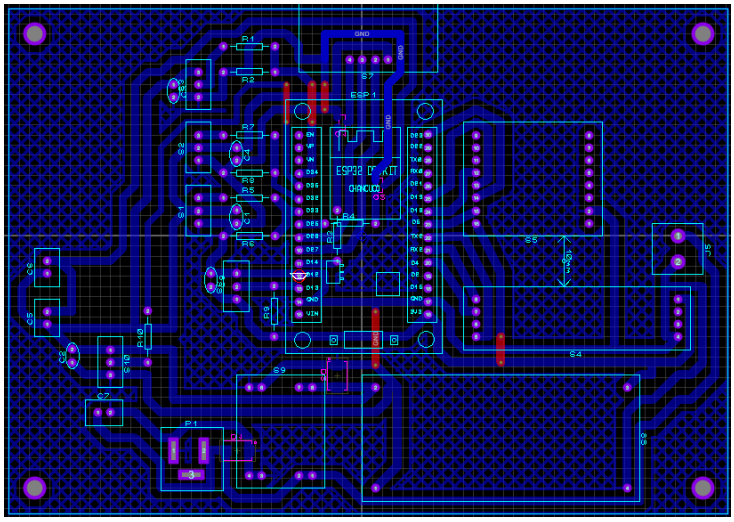

Figure 7. PCB v2

Firmware integration

Firmware integration entailed the logical synthesis of data acquisition, power management, and telemetry stacks. Validation followed a granular approach, testing each code module in isolation before deployment. Low-level drivers were scrutinized to guarantee signal fidelity across I²C and analog channels, ensuring precise transducer readings. Simultaneously, the storage routines underwent stress testing to verify that file integrity persisted even during abrupt system resets. Temporal precision was confirmed via the RTC to minimize drift in sampling intervals, while the Wi-Fi client was subjected to controlled connectivity simulations to validate its opportunistic transmission logic. Once the hardware was assembled and the operating logic fully defined, a first version of the prototype was assembled *Figure 7* for outdoor functional testing.

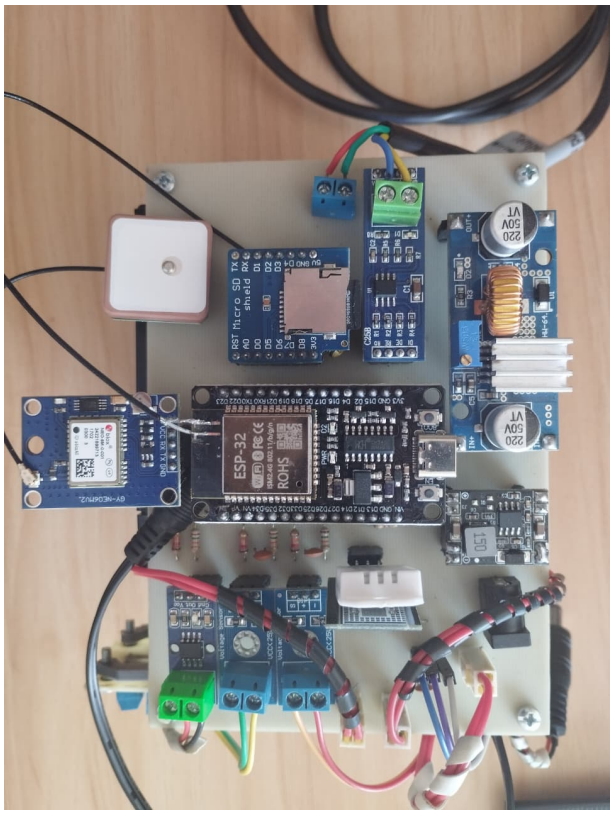

Figure 8. Interior of the prototype

Challenges Encountered and Solutions Implemented

During outdoor testing, the system was exposed to a day with hours of peak solar radiation. It had no operational problems; the sensor readings were stable and consistent, as were the power lines. The correct sizing of the solar panel for charging the battery was verified with the system running. However, after 5 hours, the system fully charged the battery. This resulted in an inaccurate reading of the solar radiation variable because, once the battery was fully charged, the current consumption of the panels tended towards 0. Since the solar radiation variable depends directly on the current factor, false zero readings were obtained, as shown in *Figure 8*.

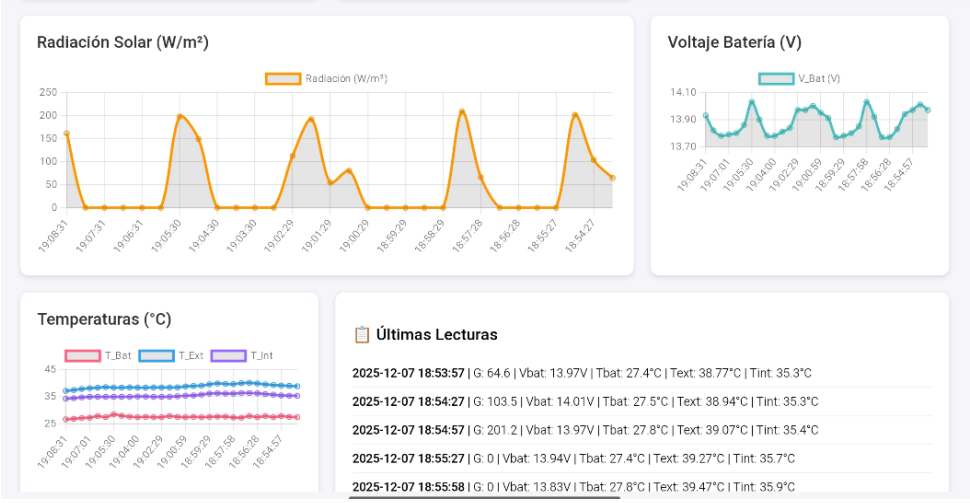

Figure 9. False 0s in solar radiation

To solve this problem, a 1-watt panel connected to a 5-watt power resistor was added. Voltage and current measurements for calculating solar radiation were taken from this circuit, thus achieving generation and consumption directly proportional to the radiation available at the time. The 15-watt panel was connected directly to the MPPT module.

3.2. Property Verification

Power Consumption Analysis and Autonomy Estimation

The electrical current consumption of the system was quantified for three representative operating conditions that characterize the energy behavior of the prototype during experimental evaluation. The measurements were made by using a previously calibrated digital multimeter, connected in series with the power supply.

The first represents the low-power condition, in which the ESP32 is kept in deep sleep mode with only the essentials being powered. Under this condition, a current consumption of 0.048 A was recorded, confirming the efficacy of the low-power design strategy and underscoring the suitability of the selected microcontroller for long-term autonomous operation.

The second condition refers to the active state, under which the ESP32 wakes up and performs a cycle of acquiring sensor data and sending information. The measured current in this case rose to 0.091 A because, during this mode, the processing unit, peripheral devices, and tasks for handling the data are already activated. Even with this

increase, consumption is still within acceptable limits for a battery-supplied embedded system.

The third operating mode is a high-demand condition-the heating pads are turned on to maintain appropriate operating temperatures in cases of low ambient temperature. Under this condition, the current consumption reached 0.259 A, which was the highest energy demand during the modes under analysis. Such a result confirms that thermal regulation is indeed the most power-consuming subsystem, although its operation is expected to be intermittent and dependent on the environmental conditions.

To estimate the system autonomy, one could consider a 12 V, 6 Ah $LiFePO_4$ battery, whose total nominal energy capacity is approximately:

$$E_{\text{battery}} = 12\,\text{V} \cdot 6\,\text{Ah} = 72\,\text{Wh} \tag{1}$$

Under a conservative operational profile, defined by prevalent low-power states, representative average current consumption was computed taking into account periodic wake-up cycles and limited activation of heating elements. For a realistic case (not considering the continuous heating activation), assume an average current of about 0.07 A. This corresponds to an average power consumption equal to:

$$P_{\text{avg}} = 12\,\text{V} \cdot 0.07\,\text{A} = 0.84\,\text{W} \tag{2}$$

Based on this average power demand, the estimated autonomy of the system operating solely on battery power is:

$$t = \frac{72\,\text{Wh}}{0.84\,\text{W}} \approx 85.7\,\text{h} \tag{3}$$

$$t_{\text{days}} = \frac{t_{\text{hours}}}{24} \tag{4}$$

$$t_{\text{days}} = \frac{85.7}{24} \approx 3.6\,\text{days} \tag{5}$$

This estimate is a conservative lower bound because photovoltaic energy input is not included. During normal operation, it is expected that the integration of the solar panel

and MPPT charge controller will substantially increase the operational autonomy, possibly even allowing for continuous operation during periods of adequate solar irradiance.

Overall, the observed consumption metrics and the resulting estimation of autonomy confirm that the proposed system architecture is energetically feasible for autonomous deployment in high-altitude environments.

Low-Temperature Battery Discharge Behavior

In order to characterize the electrical performance of the system under low-temperature conditions, a controlled experiment was conducted inside a laboratory freezer. During the test, the system was run in continuous mode while external temperature, external relative humidity, and battery voltage were recorded with timestamps. With this configuration, it was possible to analyze the effects that the environment had on battery performance during a long discharge.

During the test, the temperature outside usually stayed lower than 0 ℃, with a minimum close to –23 ℃ to represent high-altitude environments of tropical glaciers. Simultaneously, the relative humidity outside showed wide variation, roughly between 35 % and 85 %, due to joint action of cold air and condensation inside the test environment.

Collected data reveal a progressive, monotonic decline in the battery voltage over time: from the initial value near 13.5 V to values below 9 V after a few days of continuous operation. Such behavior evidences a furthered, sustained discharge process with no sudden drop and instability in voltage under low-temperature conditions.

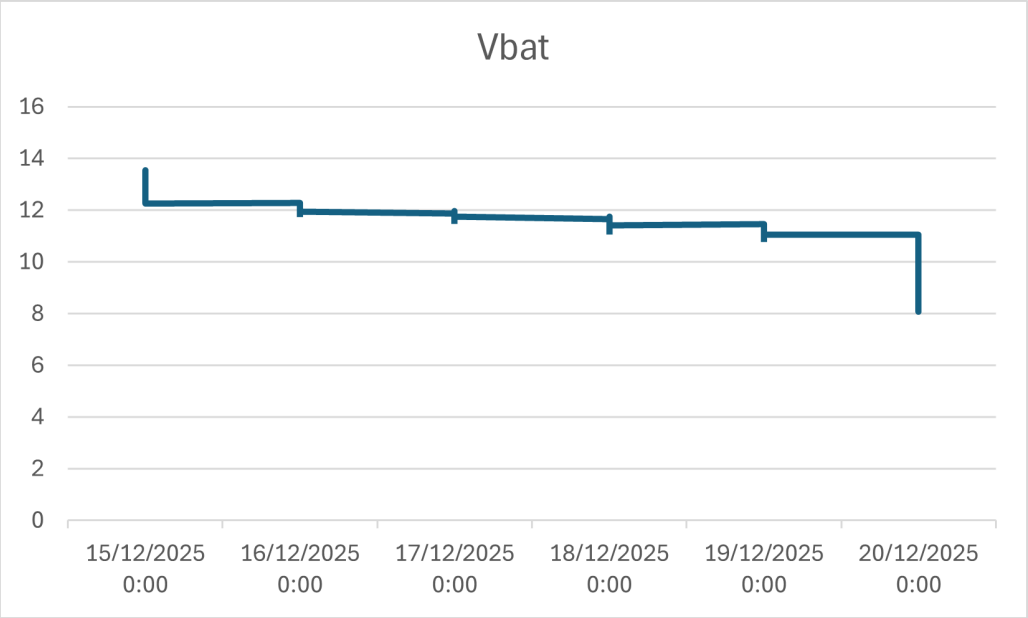

Figure 10. Battery voltage (V_{bat}) evolution during low-temperature freezer test.

A relationship between time elapsed and voltage decay is clearly observed as shown in *Figure 10*; the voltage reduces more rapidly in the initial stages of the test and gradually slows down toward the end. This trend follows the general discharge characteristics of lithium-based batteries operating at low temperatures, where internal resistance increases and effective capacity is reduced.

Solar charging

During the solar charging test, the irradiance signal starts reporting zero values after 14:00. These zeros are not associated with the absence of solar input, but with the charging process reaching its termination condition (battery fully charged and the charger limiting or stopping energy intake). Therefore, the charging analysis was restricted to the effective charging window from 07:22 to 14:00. Under these conditions, the prototype required approximately 6 h 38 min to reach 100% state of charge. The average irradiance was computed only over this interval to avoid bias introduced by post-charge zero readings.

$$t_{100\%} = t_{\text{cut}} - t_0 \tag{6}$$

$$G_{\text{avg,chg}} = \frac{1}{N}\sum_{i=1}^{N} G_i \qquad \text{for } t_i \le t_{\text{cut}} \tag{7}$$

$$P_{\text{pv,avg}} = P_{\text{STC}} \left(\frac{G_{\text{avg,chg}}}{1000} \right) \tag{8}$$

$$P_{\text{chg,avg}} = P_{\text{pv,avg}} \cdot \eta_{\text{tot}} \tag{9}$$

Cost Analysis

The total cost of the developed prototype was estimated considering locally sourced components, imported elements, and non-material costs associated with procurement and assembly. Table **??** summarizes the complete cost breakdown. Overall, the results indicate that the electronic hardware represents only a fraction of the final cost, while labor and importation dominate the total budget. This provides a realistic reference for evaluating the economic feasibility of replicating the prototype and identifies where future iterations could reduce costs through design simplification, local sourcing, or assembly optimization.

Table 2. Bill of materials and cost estimation of the autonomous monitoring system.

Units	Component	Unit price (USD)	Total price (USD)
Non-imported components			
1	DC Jack	0.5	0.5
2	FZ0430 voltage sensor	3.5	7
1	ACS712 current sensor	4.9	4.9
1	DHT22 temperature and humidity sensor	7.5	7.5
1	Buck converter 5V	2	2
1	Buck converter 3.3V	4	4
1	MAX485 RS485 transceiver	3	3
1	Micro SD card 2GB	5	5
1	SPI Micro SD module	2.5	2.5
1	ESP32 DEVKIT	10	10
1	GY-GPS6MV2 GPS module	12	12
1	LM35 temperature sensor	2.5	2.5
4	Terminal blocks	0.25	1
5	Ceramic capacitor 0.1 μF	0.1	0.5
3	Resistor 12 kΩ	0.2	0.6
2	Resistor 330 Ω	0.2	0.4
3	Resistor 15 kΩ	0.2	0.6
1	Resistor 20 Ω 5W	0.5	0.5
1	Solar panel 15 W	30	30
1	Solar panel 1 W	7	7
1	Control PCB	5.5	5.5
1	Power PCB	13.75	13.75
1	N-channel MOSFET SI2300	0.55	0.55
1	PLA filament for 3D printing	24	24

Continued on next page

Units	Component	Unit price (USD)	Total price (USD)
		Total non-imported components	**145.3**
Imported components			
1	TVS diode 18V unidirectional	0.5	0.5
1	TVS diode 6V unidirectional	0.5	0.5
1	$LiFePO_4$ battery 12V 6Ah	25	25
1	NOYITO MPPT controller	13	13
1	SHT30 PLC DCS sensor	40	40
1	Hydrophobic valve	3.5	3.5
1	WiFi antenna 2.4 GHz	4.25	4.25
2	Heating pads	0.8	1.6
2	SMA adapter	3.5	7
3	IP68 cable gland	0.7	2.1
2	U.FL to SMA cable	3	6
1	GPS antenna 1575 MHz	22	22
1	ABS IP67 junction box	20.6	20.6
		Total imported components	**146.05**
Non-material costs			
N/A	Import costs	N/A	59.5
200 h	Labor cost (USD 8/h)	8	1600
		Final total cost	**1950.85**

4. Conclusions

- The development of the autonomous monitoring system enabled the successful integration of sensing, power management, data storage, and wireless communication into a compact and functional prototype. During the design and implementation process, each subsystem (environmental sensing, battery diagnostics, powertrain, local storage, and MCU control) was individually validated and subsequently assembled into a cohesive unit capable of operating in high-altitude environments.

- Ultimately, the project achieved its primary objective: the creation of a solar-powered, autonomous monitoring prototype capable of persistently recording and promptly transmitting data. Laboratory tests confirmed the architecture's stability, validating the accurate acquisition of environmental variables, along with critical system metrics such as current and voltage. Furthermore, stress tests of the power subsystem verified that the MPPT regulation and $LiFePO_4$ storage could maintain operations indefinitely. In addition to this hardware stability, the firmware logic achieved a precise balance between deep sleep preservation, local data persistence, and conditional telemetry.

- The experimental results prove that the developed prototype can operate autonomously in controlled conditions, keeping functional continuity even at low-temperature values. Analyzing the power consumption reveals that the low-power modes of the microcontroller, along with the switching on/off of the subsystems, significantly extends functional autonomy for the system. Moreover, the discharge tests evidence stable voltage behaviors in a wide external temperature spectrum, confirming the appropriateness of the proposed power architecture for environmental monitoring in high-altitude environments.

- Analysis of the solar irradiance and the resulting charging performance confirms that the photovoltaic generation system, combined with the applied energy management strategy, is capable of fully recharging this prototype under solar irradiance conditions typical in the Ecuadorian Andes. While there were zero irra-

diance measurements after the battery was already full, the obtained irradiance profile allowed both determining the optimal energy harvesting intervals and estimating real-life achievable charging times. These findings support the conceived design of the system and confirm its feasibility as a baseline for an autonomous monitoring station that could be scaled up and improved in subsequent research efforts.

5. Recommendations

- To further extend operational autonomy, future iterations should prioritize refining energy management algorithms. Static schedules could be replaced with dynamic sampling frequencies or adaptive sleep intervals, enabling the system to react intelligently to critical battery levels. Regarding hardware, efficiency improvements could be achieved by isolating high-consumption modules using power control techniques. Furthermore, it is recommended to re-evaluate the propulsion system, specifically exploring alternative MPPT topologies and optimizing the sizing ratio between photovoltaics and storage to maximize harvest yield.

- Data integrity must be reinforced through hardware redundancy. By integrating secondary sensing nodes for temperature and humidity, the system effectively eliminates single points of failure. Furthermore, the adoption of industrial grade radiation sensors is recommended; this upgrade would not only improve accuracy but also enable the system to perform autonomous self-validation through cross-checking of readings.

REFERENCES

[1] *VDI 2206: Design methodology for mechatronic systems*, Verein Deutscher Ingenieure (VDI) Std., 2004.

[2] B. Francou, M. Vuille, V. Favier, y B. Cáceres, "New evidence for an enso impact on low-latitude glaciers: Antizana 15, andes of ecuador, 0°28's," *Journal of Geophysical Research Atmospheres*, vol. 109, no. 18, 2004.

[3] R. Basantes-Serrano *et al.*, "New insights into the decadal variability in glacier volume of a tropical ice cap, antisana (0°29' s, 78°09' w), explained by the morpho-topographic and climatic context," *Cryosphere*, vol. 16, no. 11, pp. 4659–4677, 2022.

[4] P. V. Vaca-Cárdenas, E. A. Muñoz-Jácome, M. L. Vaca-Cárdenas, D. F. Cushquicullma-Colcha, y J. Guerrero-Casado, "The recent extinction of the carihuairazo volcano glacier in the ecuadorian andes using multivariate analysis techniques," *Earth (Switzerland)*, vol. 6, no. 3, 2025.

[5] C. Manciati, M. Villacís, J. D. Taupin, E. Cadier, R. Galárraga-Sánchez, y B. Cáceres, "Empirical mass balance modelling of south american tropical glaciers: Case study of antisana volcano, ecuador," *Hydrological Sciences Journal*, vol. 59, no. 8, pp. 1519–1535, 2014.

[6] L. F. Gualco *et al.*, "Assessing the contribution of glacier melt to discharge in the tropics: The case of study of the antisana glacier 12 in ecuador," *Frontiers in Earth Science*, vol. 10, 2022.

[7] S. H. Abdulhussain *et al.*, "A comprehensive review of sensor technologies in iot: Technical aspects, challenges, and future directions," *Computers*, 2025.

[8] D. Witczak y S. Szymoniak, "Review of monitoring and control systems based on internet of things," *Applied Sciences*, 2024.

[9] A. Alshami, E. Ali, M. Elsayed, A. E. E. Eltoukhy, y T. Zayed, "Iot innovations in sustainable water and wastewater management and water quality monitoring: A

comprehensive review of advancements, implications, and future directions," *IEEE Access*, vol. 12, pp. 58 427–58 453, 2024.

A.1. Functional Architecture

This appendix presents the functional architecture of the autonomous monitoring system. It outlines the system functions and the flow of information between sensing, processing, energy management, and communication modules.

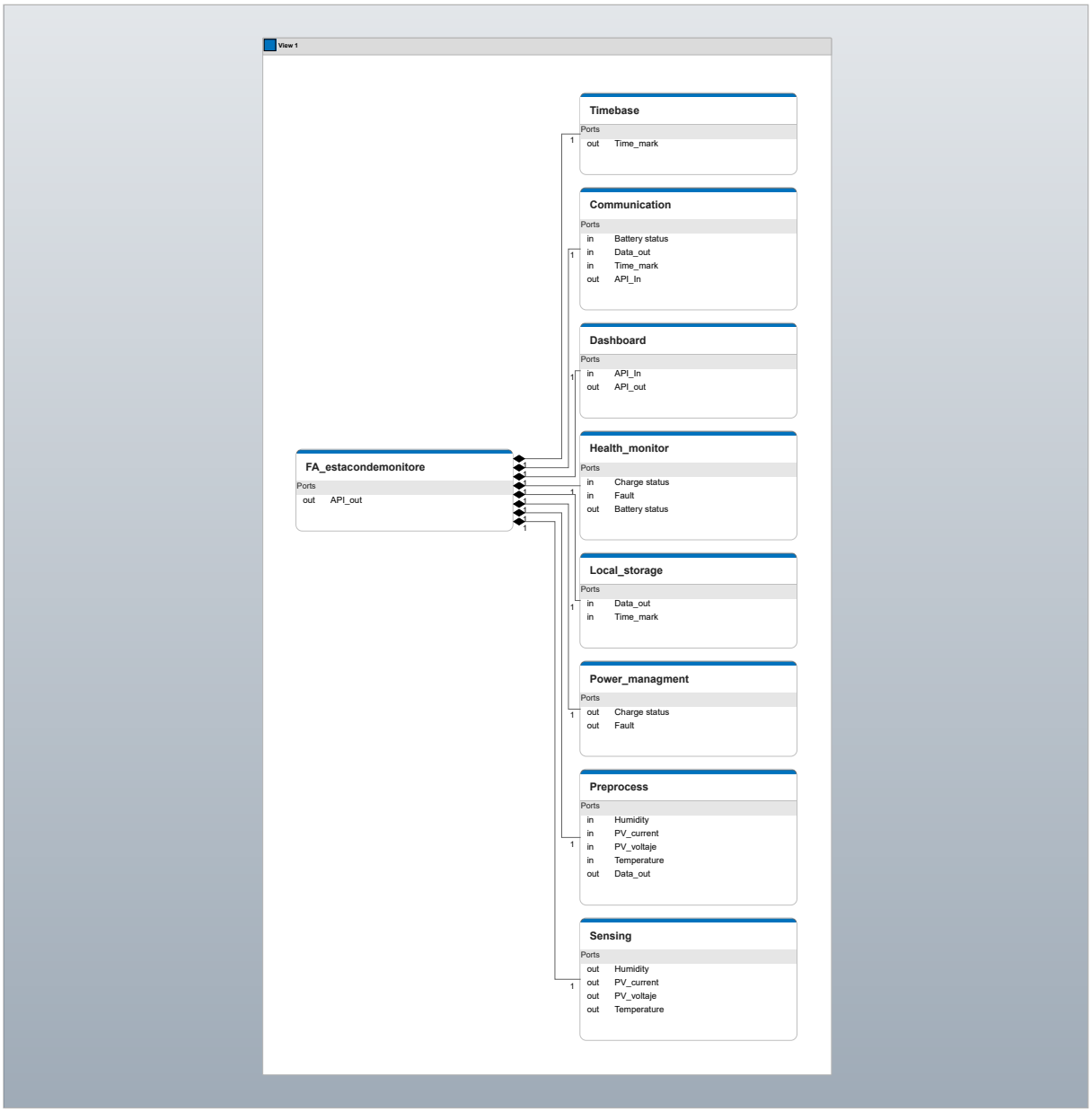

Figure 11. Functional architecture of the autonomous monitoring system.

A.2. Logical Architecture

This appendix contains the logical architecture, where the internal behavior of the system is described through its software components, decision blocks, communication routines, and data processing paths.

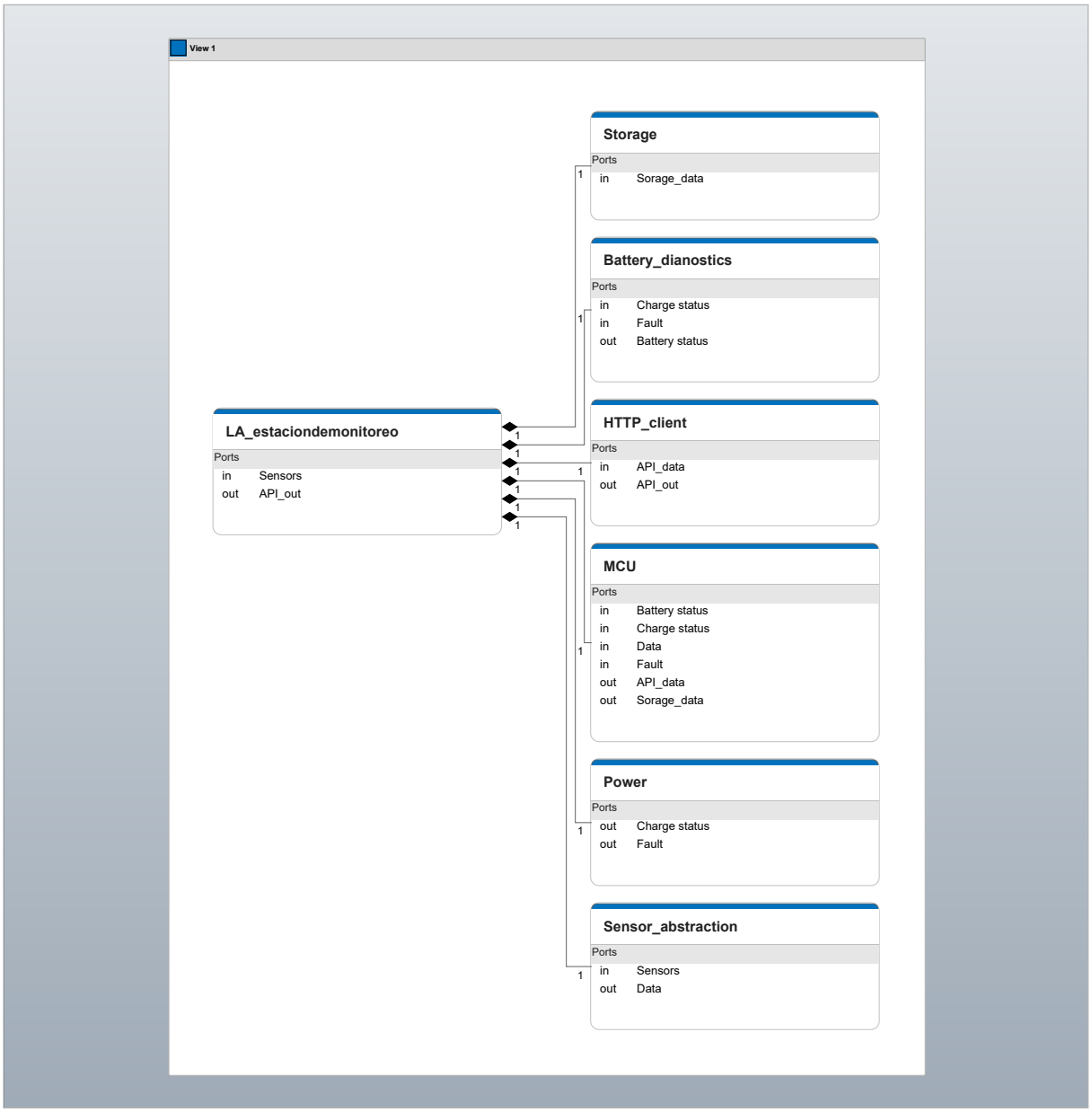

Figure 12. Logical architecture showing firmware modules, data flow, and internal system logic.

A.3. Physical Architecture

This appendix presents the physical architecture of the prototype. It shows the hardware modules, interconnections, and the physical arrangement of sensors, power electronics, and embedded components.

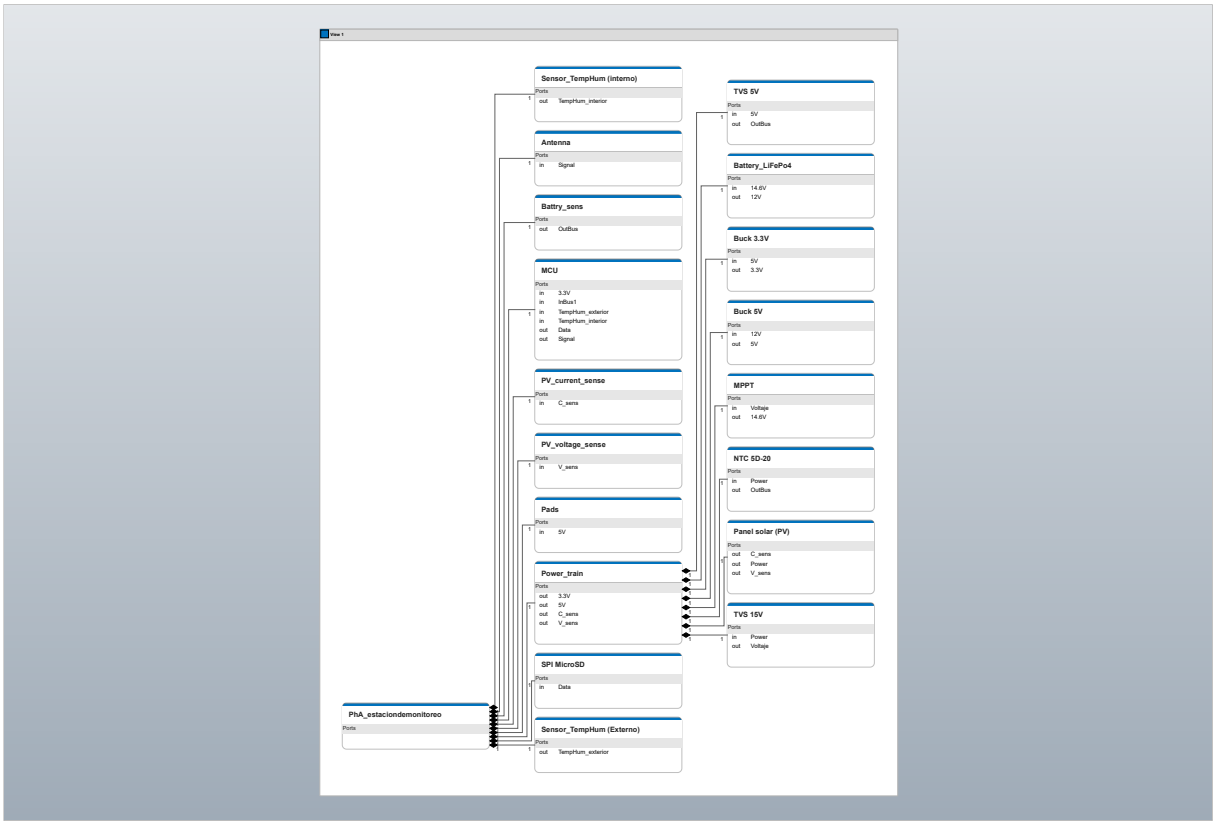

Figure 13. Physical architecture of the autonomous monitoring system.

A.4. Firmware operational flowchart

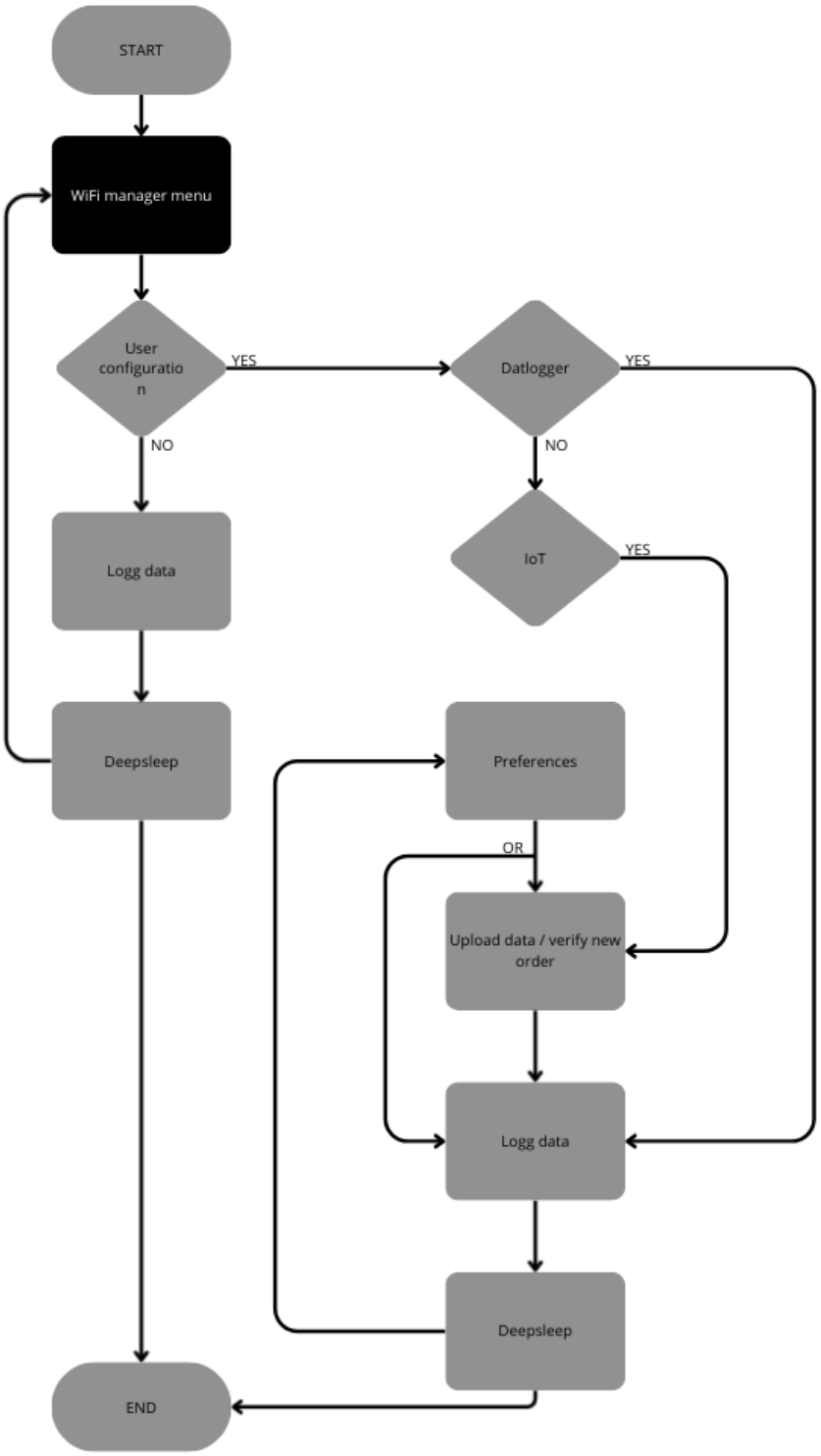

Figure 14. Operational flow of the embedded firmware: configuration stage, operating modes (Datalogger/IoT), and deep sleep strategy.